

Landslides (2017) 14:1655–1675  
DOI 10.1007/s10346-017-0811-1  
Received: 21 April 2016  
Accepted: 13 February 2017  
Published online: 21 March 2017  
© Springer-Verlag Berlin Heidelberg 2017

Anne Clayton · Doug Stead · Derek Kinakin · Andrea Wolter

## Engineering geomorphological interpretation of the Mitchell Creek Landslide, British Columbia, Canada

**Abstract** The recent assessment of the Mitchell Creek Landslide (MCL) in northern British Columbia is a good case history of engineering geomorphological analysis of a large landslide. It was completed using historic aerial photographs, with approximately 20-year time intervals dating back to the mid-twentieth century and field investigations completed between 2008 and 2014. The large bedrock slide initiated between 1956 and 1972 and continues to experience ongoing annual movements. Significant glacial downwasting and retreat has been observed in the photographic record, and it is hypothesized that alpine glaciation has contributed to development of the MCL. This paper documents four aspects of the engineering geomorphological assessment completed at the MCL: (i) topographic evolution, (ii) slope morphology, (iii) deformation features, and (iv) displacement behavior. Four distinct geomorphic zones have been defined at the MCL based on these analyses, controlled by different failure mechanisms. The extents of these zones have changed little over the documented history of the landslide, and rates of movement estimated from aerial photography have been consistent over the last 60 years. Retreat of the Mitchell Valley Glacier appears to have played an important role in landslide initiation, as the ice mass receded the kinematic freedom of the slope increased. This study of the initiation and development of the MCL demonstrates the capabilities of a multi-faceted approach to engineering geomorphology. The combination of historical aerial photographs with digital photogrammetric modeling and point cloud analysis techniques, and geomorphological mapping, allows for development of a robust understanding of landslide behavior.

**Keywords** Landslide · Geomorphology · Remote sensing · Photogrammetry · Glacial retreat

### Introduction

Landslide characterization should incorporate a wide array of geoscience techniques in order to understand the behavior of unstable masses of soil and rock (Clague and Stead 2012; Turner 1996). Factors that can lead to large-scale slope instability include slope geometry, glacial and geologic history, structural geology, geomechanical properties, hydrogeologic conditions, earthquake events, and weathering/rock damage, all of which influence the rock mass strength and applied stresses within the slope. Engineering geomorphology provides a methodology to evaluate and understand current and historic processes with surficial expressions that affect slope stability (Griffiths 2002, GSL 1972).

Several important methods have been developed that use engineering geomorphological techniques. A comprehensive summary of the history of engineering geomorphology around the world, the requisite skills of an engineering geomorphologist, and the

wide range of practical applications of the science can be found in Griffiths (2014). The Geological Society of London Engineering Group Working Party (GSL 1972) put together recommendations for a standard set of plan and section map preparation procedures including symbols for use in the UK. However, due to the complex nature of geomorphic systems, they also recommended that the practitioner at each site customize mapping symbology to highlight key features for the intended use of the map. Throughout the 1970s and 1980s, engineering geological/geomorphological mapping was recognized as important but did not play a major role in many engineering projects (Griffiths 2014). In the 1990s, engineering geology maps developed for special purposes, for example landslide susceptibility, began to appear and are now being used to guide development plans in areas with natural hazards particularly in Hong Kong (Hencher and Malone 2012). In British Columbia (BC), Canada, terrain mapping (DEGIFS 2002) has been employed in the forestry industry since the 1970s in order to evaluate and manage forest resources (Schwab and Geertsema 2010). The techniques developed in the UK are very useful when applied to landslide sites. For example, Bovis (1990) produced a large-scale engineering geology map for Affliction Creek Sackung; it includes geological contacts (bedrock), Quaternary deposits, landslide scarps, glacier outline, and creeks. Direct mapping from georeferenced imagery and visualization including slope aspect and slope angle mapping has been completed within the GIS software in the Western Italian Alps (Giardino et al. 2004) and for the catastrophic landslides at Vajont, Italy, and Madison Canyon, USA (Wolter 2014). At Vajont, Wolter (2014) used geomorphological mapping to identify zones of compression and extension in the deposit, and to evaluate the mechanics of the slide movement—identifying two main, two small, and possibly five sub-blocks within one of the main blocks with distinct movement styles. Completing an engineering geomorphological assessment at the beginning of a landslide investigation provides a large amount of information and added value to the project for a relatively small amount of effort and cost. It can also identify critical areas that should be targeted in future studies, ensuring that resources are used efficiently.

The Mitchell Creek Landslide (MCL), located in northwestern B.C., can be classified as a massive, active, composite rockslide (Cruden and Varnes 1996), or more simply as a compound rockslide (Hung et al. 2014). Our study of the MCL is an example of what can be accomplished with historic remote sensing imagery and a modern engineering geological investigation (Stead and Clayton 2014). Visible surface deformation initiated between 1956 and 1972 during rapid glacial retreat in the valley; slow deformation of the landslide is ongoing. The landslide was identified during mineral exploration in the area; several active projects are located in the Mitchell Valley and surrounding area. As a result of these studies, the geological setting of the site is relatively

well known, and this remote site is accessible for continuing engineering geological investigation. Targeted study of the landslide was initiated by BGC Engineering Inc. in 2008 (BGC 2010); field investigation and monitoring of the site has continued through 2013 in partnership with Seabridge Gold, Pretivm Resources, and Simon Fraser University. The landslide is approximately 1 km wide, 500 m high, and is actively deforming. Surficial characterization of the MCL from 1956 to present has been completed using geological data, geomorphological analysis (photogrammetric and geometric techniques), hydrological observations, and historic and modern slope monitoring. Deformation features on the slope have been mapped and analyzed. Geomorphic zones within the landslide were defined using a combination of these analyses, and deformation mechanisms within each zone assessed. Three zones were defined within the main landslide and include a lower zone that is toppling, an upper zone of sliding, and a transition zone of extension in between (Fig. 1). A fourth zone has been identified that represents a potentially unstable mass of rock above the main landslide scarp. Movement rates from 1956 to 2010 have been estimated using aerial photographs, and compared with survey monitoring for the period 2008 to 2013.

## Setting

### Regional geology

The MCL is located within the Stikinia Terrane of the Intermontane belt of the North American Cordillera (Lechner 2008). It

consists of Triassic and Jurassic volcanic island arcs that were accreted onto the North American continent during the Cordilleran Orogeny. The Mitchell Valley contains the Stuhini and Hazelton groups, both of which are composed of deformed volcanic, volcanoclastic, and sedimentary rocks that have been brecciated by intrusions and mineralized (Margolis 1993). Large bodies of Jurassic Mitchell intrusion are found on the north side of the Mitchell Valley above the Mitchell thrust fault (MTF) and on the top of the Mitchell-Sulphurets Ridge. Major fold and fault systems are present in the study area which formed during the Late Cretaceous compressional regime. Folding has been identified west of the study area in the Stuhini rocks of the McTagg anticlinorium (Campbell 2009) with fold axes striking northeast. Regional thrust faulting verges eastwards; two of these faults, the Mitchell (MTF) and Sulphurets (STF), occur in the Mitchell Valley, placing Triassic Stuhini Group rocks above Jurassic Hazelton Group rocks. The MCL is located in a sheet of Hazelton Group rocks between the two thrust faults and is composed of foliated and altered andesitic tuffs and volcanics; due to intense quartz-sericite-pyrite (QSP) alteration sometimes combined with quartz stockwork, protolith rock type can be difficult to identify. The shallow northwest dipping MTF is located approximately at the base of the instability, and the Brucejack fault (BJF), a sub-vertical fault that has experienced dextral strike-slip and normal motion, strikes north-south through the eastern Mitchell Valley, near and approximately parallel to the eastern boundary of the landslide (Fig. 1). A penetrative macroscopic cleavage occurs in most of the rocks of the Mitchell

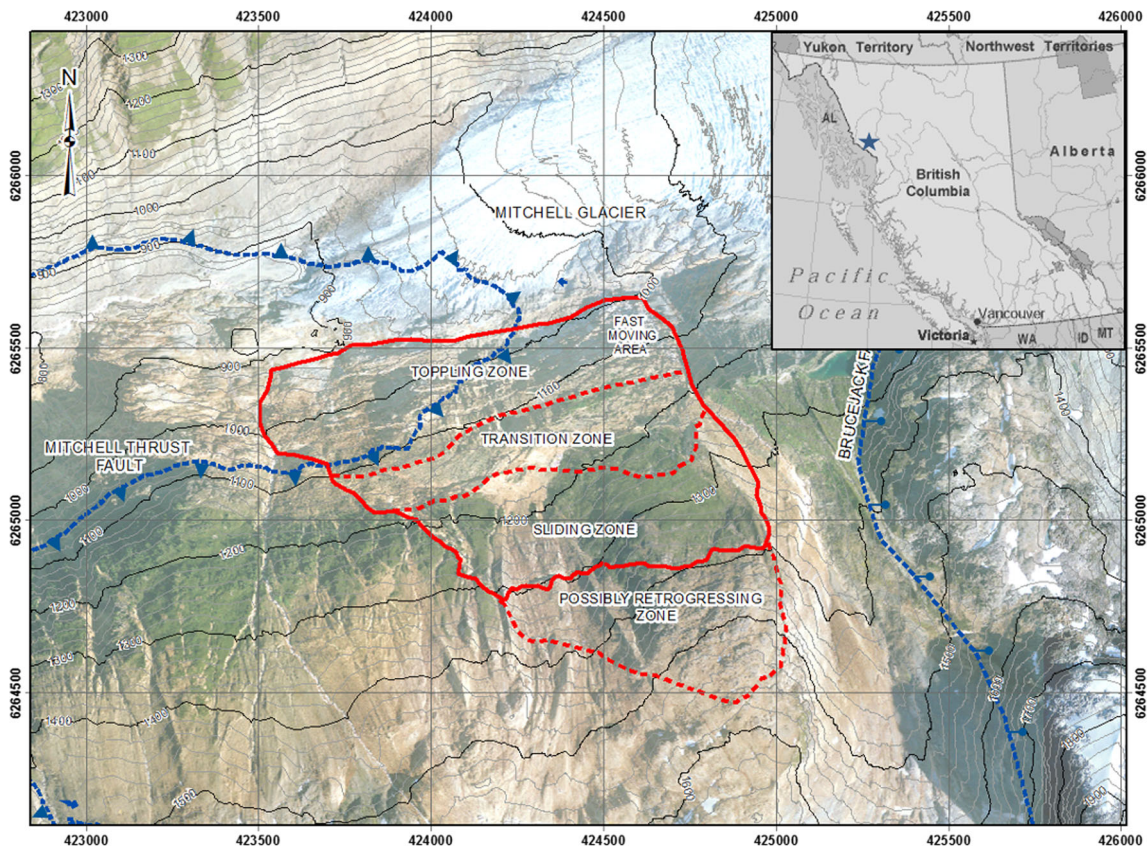


**Fig. 1** Mitchell Creek Landslide (MCL) outline in *solid red* on the 2010 ortho-photograph; geomorphic zone boundaries are indicated by *red dashed lines* and regional faults by *blue dashed lines*



Valley. The degree of foliation development is proportional to the concentration of phyllosilicates, primarily sericite and chlorite, in the rock (Margolis 1993). In the area of the MCL, the in situ foliation dips steeply (50–90°) to the N-NNE; locally, there are zones that pass through vertical and dip steeply to the S-SSW.

### Physiography, climate, and geomorphology

The east-west trending Mitchell Valley has approximately 1000 m of relief with the north wall ridge reaching over 2000 masl. Both the ridge tops and valley floor slope down to the west. The altered and mineralized rocks of the valley have experienced tectonic deformation (folding and faulting), uplift, glacial and fluvial erosion, and mass wasting. Geomorphic features in the valley reflect this history, with distinct lateral moraines related to the main valley and tributary glaciers, striated and smoothed bedrock, deeply incised gullies with debris aprons, and avalanche scars visible on the aerial photograph in Fig. 1. Of particular note with respect to the Mitchell Creek Landslide is the Little Ice Age (LIA) lateral moraine of the Mitchell Glacier located approximately 200 m above the base of the landslide. The Mitchell Creek downstream of the retreating glacial front is wide with braided gravel channels, typical of a paraglacial valley. Debris in the valley bottom approximately 2 km west of the Mitchell Creek Landslide is the result of another Holocene landslide in the rock mass of the south valley wall (BGC 2010). The climate of the area is a temperate or northern coastal rainforest, with mean annual precipitation estimated to be 1652 mm (Rescan 2009); subarctic conditions exist at high elevations. The duration of the snow-free season varies depending on elevation; for the MCL, it is approximately June through September. Spring melt and fall storms typical of coastal BC mean that there are typically two annual pulses of groundwater infiltration and surface water runoff. Multiple groundwater seeps have been observed in the lower slopes of the Mitchell Valley, on both the north and south walls, some associated with mineral precipitates (e.g., malachite and azurite) visible from across the valley.

Deglaciation of the Mitchell Valley is ongoing and is believed to be a key factor contributing to landslide evolution. Rates of retreat have been estimated on the order of 30 m/year for the past 30 years, and single-year retreats of greater than 50 m have been observed in the last decade. Considerable thinning of the remaining glacier has occurred over the same time period exposing fresh rock slopes and removing a kinematic buttress to landslide motion.

### Methods and materials

Historic aerial photographs were used for photogrammetry, engineering geomorphological mapping, identification of deformation features, and displacement tracking. Detailed surface mapping was completed in 2013 with a focus on deformation character interpretation and structural mapping.

Three-dimensional topography models were built from the 1956, 1972, 1992, and 2010 aerial imagery using the 3DM suite of software developed by Adam Technology (2013). Changes in landslide geometry between the models have been identified and zones of accumulation and depletion delineated. Using ESRI ArcGIS (2013), the older aerial photographs were georeferenced to the 2010 imagery by matching points outside of the landslide area assumed to be stable. Geomorphological features over the landslide area including concave and convex slope breaks, cliffs, glacial

moraines, hydrogeologic features, and permanent snowfields have been mapped for each set of aerial photographs. Deformation features were mapped in GIS on the georeferenced aerial photographs. Movement styles in the landslide mass have been identified using orientation and length of the deformation features and geomorphological character - this has been used to divide the project area into four major zones. Connections between the timing of major events in the valley, e.g., glacial retreat and landslide initiation, have been considered. Within the landslide, distinct natural targets were digitized from each aerial photograph to estimate displacement magnitude and rate; relative accelerations and decelerations were noted. The results of these analyses have been synthesized into a conceptual model of slope evolution. Details of the four methods used to evaluate the MCL are described in the following sections.

### Photogrammetry

Photogrammetry techniques were used to recreate the topography for each set of aerial photographs. Four sets of aerial photographs captured over the last 60 years were used to complete photogrammetric analysis of the Mitchell Creek Landslide. The photographs date from 1956, 1972, 1992, and 2010; the three oldest sets were taken by the provincial government of British Columbia, and the 2010 photographs were taken by AeroGeometrics Ltd. Three-dimensional analysis was completed using photogrammetric techniques on aerial imagery of the Mitchell Creek Landslide to create geospatially referenced point clouds and Digital Terrain Models (DTMs) for each set of photographs. Basic camera information, e.g., focal length and sensor size, for the photographs was provided by the B.C. Government and AeroGeometrics Ltd. Twenty stable natural control points in the Mitchell Valley in the 2010 images were selected to geospatially reference the models. These points were digitized in GIS and draped over 2010 LiDAR data to obtain co-ordinates. In each of the sets of historic photographs, those control points that could be identified were used to geospatially reference the models and to calculate camera calibration data for use in 3DM CalibCam (Adam Technology 2012). A summary of input photograph characteristics and resulting model parameters is provided in Table 1. Vegetation cover, shadows, and the resulting lack of texture in the mid-slope in both the 1956 and 1972 photographs meant that the photogrammetric software could not identify many matching points over the area and therefore did not generate points within relatively large areas of the interior of the landslide. In the 1992 and 2010 photographs, this was not a problem because of higher quality imagery and an increase in surface texture due to landslide deformation; therefore, the generated point density over the landslide area is relatively consistent without any missing areas.

The DTM models were compared using a tool in 3DM Analyst to create a DTM difference map. This tool calculates the absolute distance from each point in one model to the nearest point in the second model by expanding a sphere from each point until it intersects the second model; it does not indicate the direction of the change between them.

While the DTM difference analysis allows for a quick visual interpretation of changes between the DTMs generated for the MCL in 2010 and 1992, in order to assess material depletion and accumulation resulting from landslide motion and vectors of

Table 1 Summary of photogrammetric model generation parameters

Image info		Photogrammetry Info					
Date	Attributes	Ground pixel size (m)	Control point accuracy (m: x,y,z)	Image accuracy (pixels)	Total RMS (m)	Point density (pts/m <sup>2</sup> )	Model comments
2010	Color 1:15 K	0.33	1.5, 1.7, 2.0	0.15	3	0.26	<ul style="list-style-type: none"> <li>- 22 control points</li> <li>- Mostly even point distributions, some blanks due to snow and shadows</li> </ul>
1992	Color black and white 1:15 K	0.26	2.4, 2.0, 4.8	0.2	5.7	0.13	<ul style="list-style-type: none"> <li>- 13 control points</li> <li>- Good agreement with 2010 model near landslide area</li> <li>- Some distortion of models near image edges, camera calibration not perfect</li> </ul>
1972	Black and white 1:30 K	0.67	1.0, 0.8, 1.7	3	2.2	0.20	<ul style="list-style-type: none"> <li>- 16 control points</li> <li>- Poor camera calibration</li> <li>- Point distribution is uneven, blank spaces in model due to image quality issues</li> </ul>
1956	Black and white 1:30 K	0.50	1.9, 1.0, 2.3	0.4	3.4	0.13	<ul style="list-style-type: none"> <li>- 12 control points</li> <li>- Apparent systematic lower elevation over landslide area compared to other photogrammetry models</li> <li>- Point distribution is uneven, blank spaces in model due to image quality issues</li> </ul>



displacement, more advanced point cloud comparisons must be made. In order to do this, point clouds generated during photogrammetric analysis were compared using Polyworks (Innovmetric 2013), an advanced spatial analysis software designed to deal with large point cloud datasets, such as those produced by laser scanners or photogrammetry models. The stable zones in the point clouds can be aligned using this code to remove slight rotations or other offsets between the models. Multiple comparison schemes are available in this software package, the most commonly used are (i) distance to closest point, which finds the closest point in cloud 2 to each point in cloud 1 and calculates the distance between them, and (ii) change in elevation, which begins with a point in cloud 1 and calculates the vertical distance between it and the point above or below it in cloud 2. Comparisons were made between each of the generated topographic models of the MCL area, beginning with 1956 and 2010—a period beginning before initiation of movement to capture the entire lifespan of movement documented to date.

### Slope morphology

Several types of geomorphological analysis and interpretation have been applied to the MCL based on the standards proposed by the Geological Society of London: Engineering Group Working Party (GSL 1972): (i) morphological or morphometric maps have been generated, documenting slope geometry for both pre-deformation and current topography; (ii) morphographic interpretation of the slope has been carried out to separate the MCL area into morphological (or landform) units considering composition of the slope and geological history of the area; and (iii) slope processes (deformation, erosion, deposition) that have acted in the past or are presently acting on the slope have been identified (Table 2).

Aerial photography and field mapping were combined to identify geomorphic zones within the landslide. Using the method and symbol recommendations from the Geological Society of London (1972), slope scale geometric—or morphometric—features were mapped on the 1956, 1992, and the 2010 photographs.

An analysis of roughness of the slope topography was completed using block statistic functions available in ArcGIS (ESRI 2013). Slope angle and aspect data derived from the 2010, 1992, and 1956 photogrammetric models were used to generate maps of mesoscale (10s to 100 s of meters) roughness of the landslide surface. Roughness

blocks 10 and 20 m square (with areas of 100 and 400 m<sup>2</sup>, respectively) were assessed for the range of values and standard deviation of the slope angle and aspect. Input DEMs had 2 m (1992 and 2010) and 5 m (1956) resolution; block sizes considered must be multiples of these values and contain enough points to evaluate the roughness of the slope. Larger blocks, e.g., 50 m, smoothed the data to an extent that landslide features were not clearly visible.

### Deformation features

Visible deformation features including normal and counterscarps, trenches, and lineaments were mapped and analyzed spatially on the 1972, 1992, and 2010 aerial photographs in ArcGIS. A classification system was developed to differentiate between major and minor features, and between normal and anti-slope movements (Table 3). Ground truthing of movement style of the features mapped on 2010 photographs was completed in 2013. For features on the older photographs, comparison of the feature networks with geomorphic zones and across time steps was completed as a check on visual mapping. The length and orientation of mapped features, by time period, were analyzed.

Spacing and persistence of major deformation features in the 1992 and 2010 imagery have been estimated in each of the landslide zones. Apparent spacing has been measured perpendicular to strike of the deformation features, approximately parallel to landslide motion for the majority of the sets. In the toppling zone, the information from 1992 photographs is often more reliable than 2010 — the eastern corner in 2010 is essentially rubble, and there are shadows obscuring some faces.

### Point displacement monitoring

Surface displacements were evaluated using the aerial photographs (1956–2010) and recent survey monitoring (2008–2013). Georeferenced historic photographs were used to evaluate horizontal slope movements: natural targets visible in all or most of the images in the four landslide zones were selected; several points in the stable ground were also selected to estimate the magnitude of georeferencing and digitizing error; plan distance and azimuth of movement between time steps was calculated for each point; total displacements with time have been estimated. Geotechnical monitoring, which began in 2008, has been compared with these average historical rates, and a benchmark established for landslide

**Table 2** Engineering geomorphology symbols

Feature classification	Description
Ridge crest	- Topographic lineament with ground sloping away in opposite directions on either side e.g., glacial moraine
Cliff	- Marks the top of steep, >45°, ground within a dip slope or an asymmetrical ridge - Used to indicated closely spaced convex and concave slope breaks separated by a scarp face
Convex slope break	- Abrupt steepening change in slope dip
Convex slope change	- Gradual steepening change in slope dip
Concave slope break	- Abrupt shallowing change in slope dip
Concave slope change	- Gradual shallowing change in slope dip
Gully	- Trough formed at intersection of slopes dipping towards each other - Used on its own to indicate narrow steep-sided valleys, together with slope break/change symbols for gentle valleys
Slope direction	- Indicates direction of magnitude of maximum slope dip

**Table 3** Deformation feature classes

Classification	Description
Main scarp	- Defines the boundary of the main slide mass
Major normal scarp	- Normal movement indicators - Large movements have been accommodated separation across scarps visible - Secondary raveling of scarp walls may have occurred
Minor normal scarp	- Normal movement indicators - Secondary scarps - Little or no separation between hanging wall and footwall
Major counterscarp	- Anti-slope movement indicators - Large movements across high an steep scarps - Troughs behind scarps may be water retaining features - Secondary raveling/detachment of blocks may occur along features
Minor counterscarp	- Anti-slope movement indicators - Secondary scarps, may connect/cross cut major features - Low relief across scarps, shallow depressions on upslope side of scarps unlikely to be water retaining
Crack/lineament	- Linear features within landslide area - Movement style unclear - Includes visible geologic structure

movement rates at the MCL. Glacial downwasting was tracked through time using the photogrammetric topography; the elevation of the midpoint of the glacier outboard of the middle of the MCL was estimated through time.

### Results of engineering geomorphological analysis

#### Topographic evolution through photogrammetry

In the 1956 photographs, there is no evidence of surface deformation in the area of the Mitchell Creek Landslide; however, by

1972, there is visible surface deformation. Comparisons between each of the generated topographic models of the MCL area capture the entire lifespan of visible surface movement. They show incremental subsidence of the mid-slope bench and deformation of the lower toppling slope between each of the models, and significant downwasting of the Mitchell Glacier. Changes in elevation of the midpoint of the glacier adjacent to the landslide have been tracked and are discussed below. Photogrammetry analysis supports the conceptual model developed during initial landslide assessment (BGC Engineering Inc. 2012).

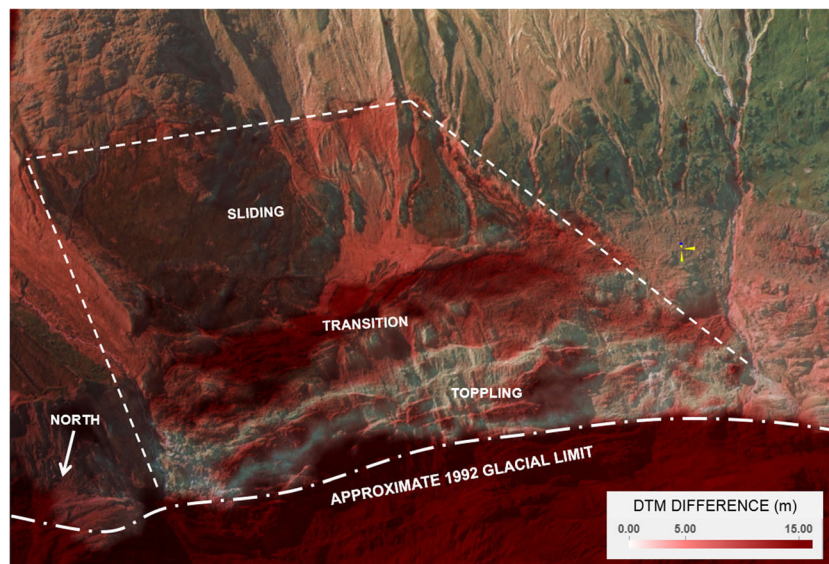


**Fig. 2** Oblique view of DTM difference map created in 3DM Analyst showing negative changes in the ground surface between 1992 and 2010 aerial photographs in meters, imagery shown from 2010

Three distinct areas are identified from the 1992–2010 DTM difference map (Fig. 2):

- The upper sliding zone has displaced up to 5 m in an apparently vertical direction between 1992 and 2010;
- The mid-slope bench represents a transition zone that has displaced 5 to 15 m with visual displacement occurring both vertically and to the north; and,
- The lower toppling zone. The DTM difference tool assessment of displacements in this zone is not as good an indicator of the true landslide motion compared to the other two zones due to the more complex deformation style of the lowest part of the slope. Estimated displacements in this zone reflect a combination of the effects of bulging of the slope due to toppling, erosion of unconsolidated glacial sediment aprons as the Mitchell Glacier retreated, and rock fall/talus apron build-up from the steep slopes.

Further analysis of the high-density point clouds of the 1992 and 2010 photogrammetry models provide a very detailed interference map for that 18-year period (Fig. 3). The edge of significant landslide movement at the main backscarp is clear with a 2 m minimum displacement cut-off. This cut-off was selected based on observed differences in stable areas. Maximum estimated displacement is 30 m. The Mitchell Glacier has receded significantly more than 30 m, and a fringe of large subsidence reflecting that is visible at the glacier edge. This analysis was able to differentiate between subsiding and bulging areas, and refine georeferencing of the historic models to the most recent 2010 point cloud.

Unfortunately, due to image quality and vegetation cover in the 1956 photographs, which resulted in a less dense point cloud than the 2010 data, the interference pattern generated by comparing the closest points between the two clouds shows only coarse changes in topography. Confidence can only be placed

in model topography differences greater than 5 m based on the variation in slope geometry apparent between the models on the stable slope west of the landslide: Because the models were built using control points that assumed this area has been stable over the past 60 years, this is a reasonable cut-off for observable landslide displacement. The maximum magnitude of subsidence observed in this comparison on the LIA moraine located mid-slope in the landslide is 45 m with bulging in the eastern half of the toppling slope of up to 20 m. Over the western half of the toppling zone, any bulging that may have occurred is obscured by glacial retreat and erosion of unconsolidated sediments present in 1956. It is important to note that despite challenges in creating a high-quality model of the 1956 topography, the general behavior of the slope between 1956 and 2010 can be observed in this comparison of the topographic models due to the large displacements that have occurred in the toppling and transition zones.

### Slope morphology

1956 provides a snapshot of the slope geometry prior to the initiation of landsliding, and the high-quality 1992 and 2010 aerial photographs allow for detailed analysis and comparison of features within the landslide. DEMs produced from photogrammetric analysis, hydrogeologic features, and Quaternary history of the site were used to identify gentle and abrupt slope breaks, slope dip direction, and valleys/gullies. From the DEMs raster maps of slope dip (Fig. 4b), slope aspect (Fig. 4c), and a hillshade representation of topography (Fig. 4d) were created to aid in delineating these features. Maps of the morphometric features are presented in Fig. 5a (1956), 5b (1992), and 5c (2010), and a symbolic legend can be found in Table 2.

Pre-slide geomorphic processes on the south slope of the Mitchell Valley include fluvial erosion and deposition, gully, snow avalanches, and glacial retreat. Fluvial erosion is primarily occurring in the upper slopes, deposition is occurring behind the

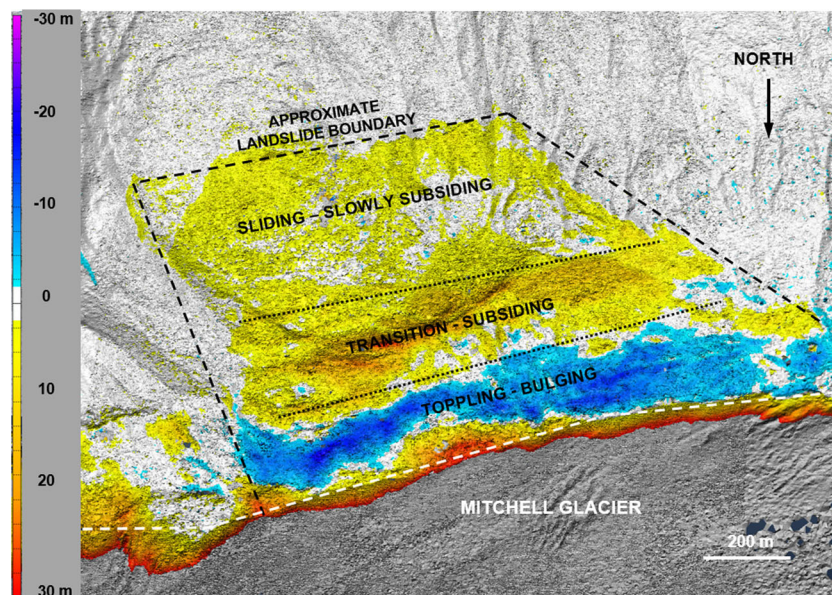


**Fig. 3** Point cloud comparison of 1992 and 2010 photogrammetric models. Distance in meters to the closest point is shown, maximum value of 30 m. Positive values (yellow–red) indicate subsidence from 1992 to 2010, negative values (blue–purple) indicate bulging/uplift



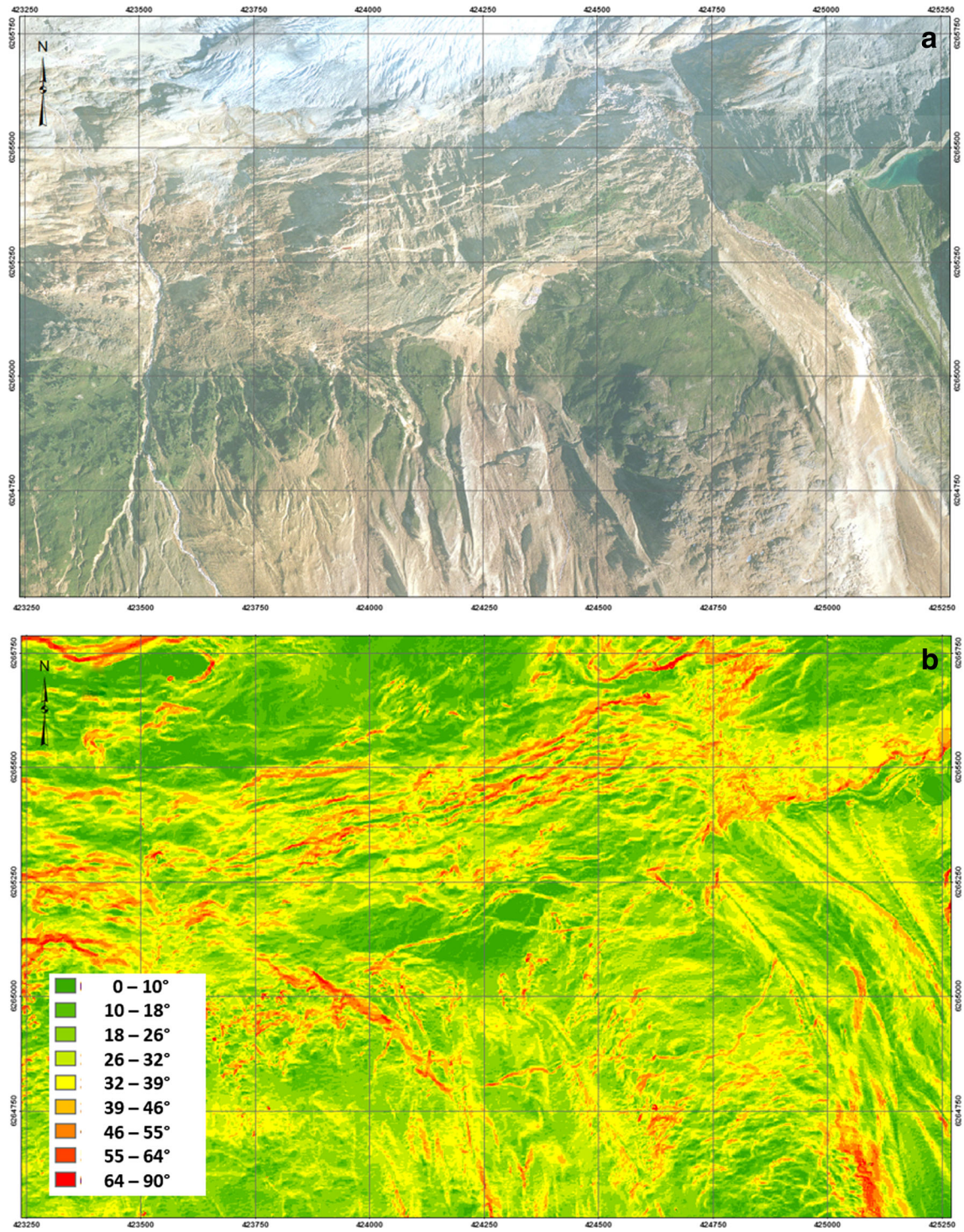


**Fig. 4** 2010 maps used in visual delineation of morphometric features: a aerial photograph, b slope angle, c slope aspect, and d hillshade

LIA maximum moraine and downstream of the glacial front. Gully incision of soil and bedrock slopes and snow avalanche activity is occurring on all of the steep slopes, along both the south and north valley walls. The gullies are generally 5 to 20 m across, and up to 50 m deep; they are typically perpendicular to the valley walls (striking N-S) on the south side of the Mitchell Valley, and on the north side are oriented either perpendicular to the valley, ENE-WSW, or a bilinear combination of the two. Glacial retreat is

ongoing in the Mitchell Valley, and was well underway in 1956; the maximum LIA moraine is located at approximately 1200 masl at the midpoint of the future MCL, and glacial midpoint elevation outboard of the same point in 1956 has been estimated from photogrammetric analysis at 1125 masl. Rates of retreat since 1980 have averaged 30 m/year, and downwasting approximately 2 m/year. Tributary glaciers from the Mitchell-Sulphurets ridge had completely retreated from the landslide area by 1956. The tip



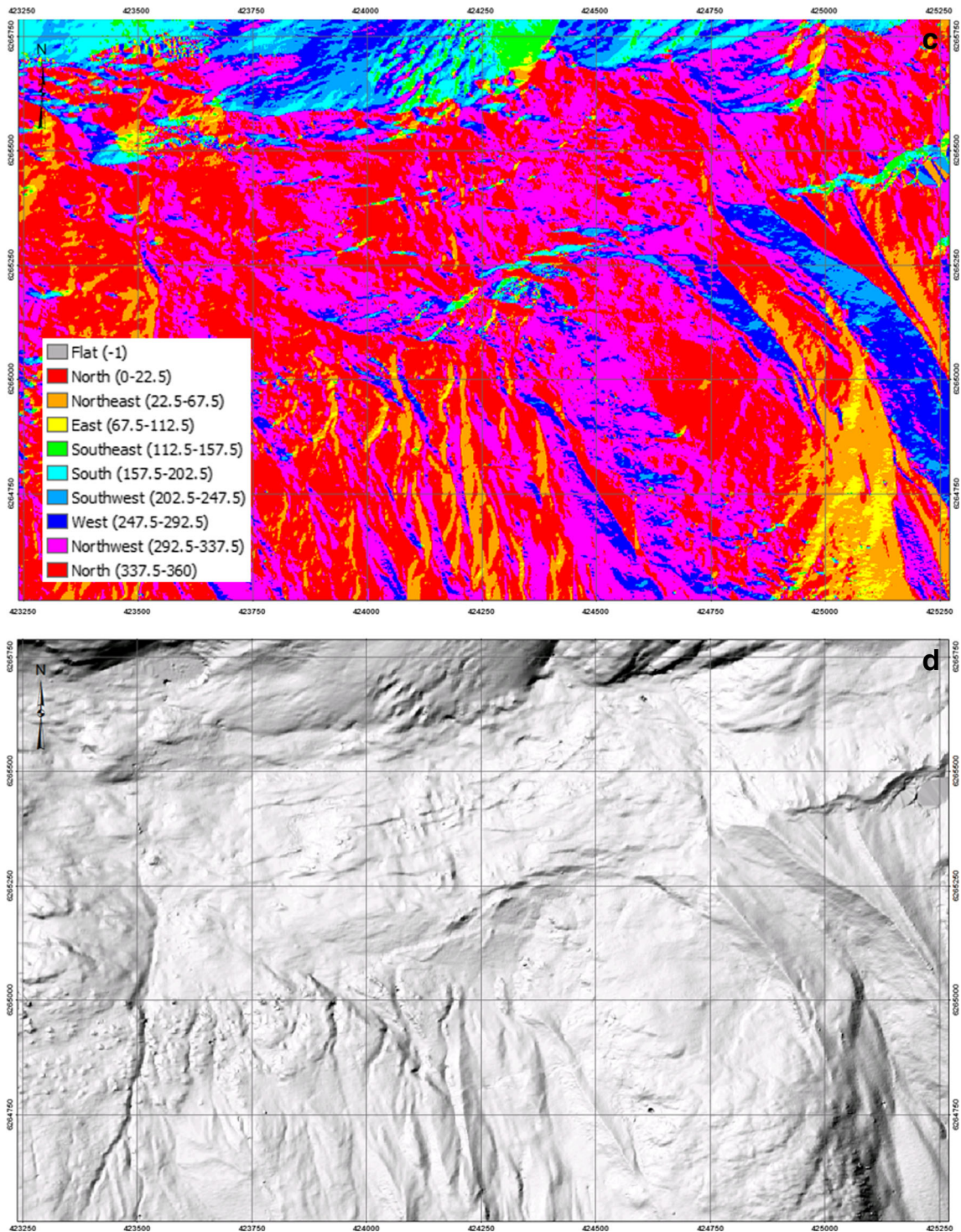


Fig. 4 (continued)

of the glacier in the Brucejack fault valley may have been at approximately the elevation of the main landslide backscarp in 1949; however, snow cover in the photographs obscures the extent of glacial ice. A glacially dammed lake is present behind the LIA lateral moraine east of the future MCL. Convex and concave slope breaks, ridges, gullies and slope direction are marked on the 1956 imagery in Fig. 5a. The area of the Mitchell Creek Landslide contains two main sets of topographic features; the first parallels

the valley walls and is visible on the slopes where bedrock is exposed or covered by a thin blanket of surficial material. This set of features displays low amplitudes and is interpreted to be due to structurally controlled erosion, parallel to the strike of the regional foliation (approximately east-west). The second set of features is related to the most recent pulse of glaciation and overprints the first (Fig. 5a). Lateral moraines from both the main Mitchell Valley Glacier and two tributary glaciers originating on



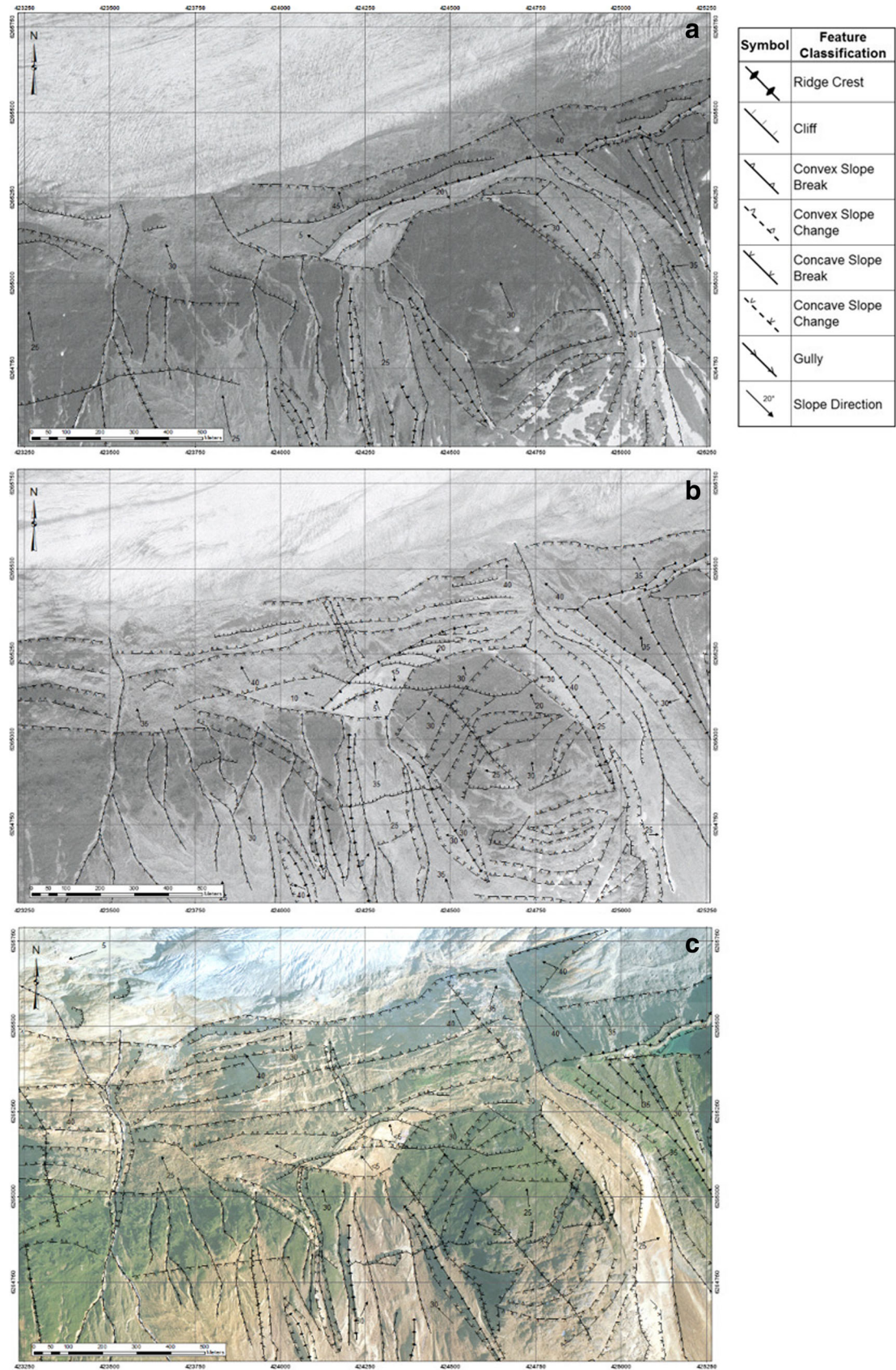


Fig. 5 Engineering geomorphology analysis morphometric maps: a 1956, b 1992, c 2012



the Mitchell-Sulphurets ridge which flowed down to the north to join the main Mitchell Glacier form prominent ridges that are 10 to 30 m high and up to 100 m across, and glacial sediments of varying thickness are present on the slope. Vegetation has not reestablished within the footprint of LIA maximum glacial extent. The steepest topography of the project area, bedrock cliff faces dipping 60–80°, is present in these recent glacial scars (Figs. 4b and 5a–c). Permanent snowfields are located above the landslide area on the Mitchell-Sulphurets ridge.

Geomorphology of the slow moving MCL changed gradually over the 60 years of record provided by aerial photographs. Geomorphic processes active in the area in 2010 continue to include fluvial erosion and deposition, gullying and snow avalanches, and glacial retreat; additionally, subsidence in the upper to mid-landslide and bulging of the lower slope are ongoing within the landslide. The midpoint of the Mitchell Glacier at the approximate landslide center has retreated from approximately 1125 masl in 1956 to approximately 1015 masl in 2010. As of 2010, there is no glacial ice abutting the landslide and the elevation of the edge of the glacier is approximately 950 masl. The lake dammed by the LIA lateral moraine of the Mitchell Glacier east of the landslide is unchanged from 1956, an indication of the stability and hydrogeological conditions of the southern valley wall outside of the landslide area. Few changes in the slope geomorphology are evident outside of the landslide zone between 1956 and 2010; bedrock slopes were exposed by glacial retreat, and a braided floodplain developed downstream of the toe of the Mitchell Glacier. Movement of the landslide is evident as:

- Slope bulging in the lower third of the mass as shown in the point cloud analysis, this is the location of the steepest recently de-glaciated slope
- Significant extension and down-dropping of the middle third or mid-slope bench/LIA moraine mid-slope bench
- Translation of the upper third of the landslide mass downward and into the valley

Scarps ranging from 1 to 15 m in height have developed at the upper limit of the main landslide and throughout the mid-slope, and counter or anti-slope scarps have developed in the bulging lower slope (Fig. 5c). The main backscarp of the landslide averages between 5 and 10 m in height within both rock and soil materials; the backscarp dips between 35 and 80° to the north and is relatively continuous across the approximately 1000-m-wide landslide mass. In the mid-slope, there are several major scarp features that range from 5 to 15 m in height, the longest of which extends 600 m. Counterscarps in the lower slope are typically 5 to 10 m wide and extend 50 to 200 m along strike.

During the period from 1992 to 2010, the landslide experienced significant geomorphic change. The character of the slide area in 1992 was dominated by pre-existing geomorphic elements (Fig. 5b), while in 2010 the geomorphology is increasingly dominated by landslide processes (Fig. 5c). The most striking example is the LIA moraine ridge, which in 1992 is easily recognizable with a south dipping slope behind the ridge, despite normal scarps striking E-W that disrupt its surface (Fig. 5b). In the 2010 photographs, the moraine is cut by multiple sets of scarps, and the former ridge is no longer a

distinct feature. Other notable changes to the geomorphology include:

- The graben defining the western edge of the sliding block has deepened and widened.
- The blocks within it are much more disturbed in 2010.
- The scarp height and the length of major features have increased.
- Minor features have developed between the major scarps of 1992.

Activity in the landslide can be divided into four zones of consistent deformation processes; the approximate location of each zone is shown on Fig. 1. Beginning at the base of the slide, there is a steep toppling region that is characterized by counterscarps, dislodged blocks, and talus (Fig. 6i, j). This zone contains numerous ground water seeps, particularly in the lowest elevations where the built up talus cones are completely saturated (observed in August 2013). A sub-region within the toppling slope has been identified comprising a highly disintegrated rock mass with potentially faster movements distinguishing this area from the rest of the toppling zone, shown in Fig. 1. This sub-region of the zone is located at the intersection of the Brucejack and Mitchell Thrust faults and may have been more tectonically damaged prior to the onset of landslide movements. It is also at a point where the Mitchell Glacier completes a 40° bend and the slope could have been subject to increased plucking, abrasion, and water pressures during glaciation.

Above the toppling zone is a region of increased density of surface deformation that coincides with the LIA lateral moraine and marks the transition from primarily toppling below to the sliding zone above. Large blocks, 5 to 60 m across, of down-dropped material characterize this zone, together with cross-cutting and complex deformation features. Scarps separating the blocks are typically 5 m high and range in length from 30 m up to 600 m. In this zone, the movement direction on the primarily normal scarps is down towards the north, but some counterscarps are also present, particularly on the western edge of the zone. The fluvial fan located in this zone may be relict, with water flow being diverted in the zone above. These features indicate a zone that is extending and subsiding, in response to removal of support by displacement of the faster-moving toppling zone below.

The sliding block above the mid-slope bench is characterized as a relatively intact block sliding along the landslide rupture surface; scarps exhibit normal movement indicators and follow pre-existing structural features. Vegetation covers most of this zone; it includes sub-alpine shrubs and grasses with the occasional stunted but upright coniferous tree. A well-developed east-west trending backscarp, 5–10 m high and 800 m long, defines the upper boundary of this zone, characterized by a cliff variably consisting of bedrock and glacial sediments. To the west the landslide boundary is a steep-sided graben up to 30 m deep and 50 m across, oriented southeast–northwest. It contains disturbed rock blocks that have detached from the main sliding block and backscarp. The eastern edge of the sliding zone is partially obscured by lateral moraine deposits associated with the now extinct Brucejack tributary glacier.



**Fig. 6** 2013 field photos from Mitchell Creek Landslide area: **a** and **b** show the backscarp above the sliding block and surface water entering the slope through a crack just above the backscarp; **c** and **d** deformation above the main landslide boundary; **e** a graben associated with the western backscarp; **f–h** the complex deformation in the transition block; and **i** and **j** foliation-controlled toppling near the base of the landslide

Above the main backscarp bedrock relaxation features have been observed. This zone may be part of ongoing retrogression of the Mitchell Creek Landslide. Possible deformation features were identified on 2010 aerial photographs; field work in 2013 confirmed the presence of these features. Open cracks, sinkholes, and normal style movement indicators (e.g., downslope movement along discontinuities, structure opening parallel to the slope contours) were observed in the field (Fig. 6a–f). The open cracks ranged from 2 to 40 cm wide, typical opening widths were 10–20 cm, with lengths ranging from 3 to 50 m and typical visible depth of 5 to 10 m. Sinkholes observed were up to 2 m deep and 1.5 m in diameter and partially debris filled. The edges of this zone have been estimated by combining the 2013 field observations, 2010 photographs, and three-dimensional visualization using Google Earth (September 2010 imagery).

Bedrock instability exists in the Brucejack fault valley at the edge of the relaxing/retrogressing upper MCL block: the nearly 100 m-high cliffs of the western wall are toppling into the tributary valley. This is interpreted to be related to glacial over-steepening in the Brucejack tributary glacial valley, and not a part of the MCL. During the 2013 field season, large blocks, 5 to 10 m across, were observed broken off and displaced eastwards.

Major features identified in morphometric mapping of the surface of the slide are discernable in each set of roughness maps (Fig. 7a 1956, b 1992, and c 2010) although the topography data from 1992 appears to be smoother than that from 2010 and 1956 which may be an artifact of the photogrammetric data processing. Outside of the main landslide mass, slope angle roughness for the northern slope is lower than the south slope of the Mitchell Valley, with only large gullies breaking the slope. Rocks of the north valley



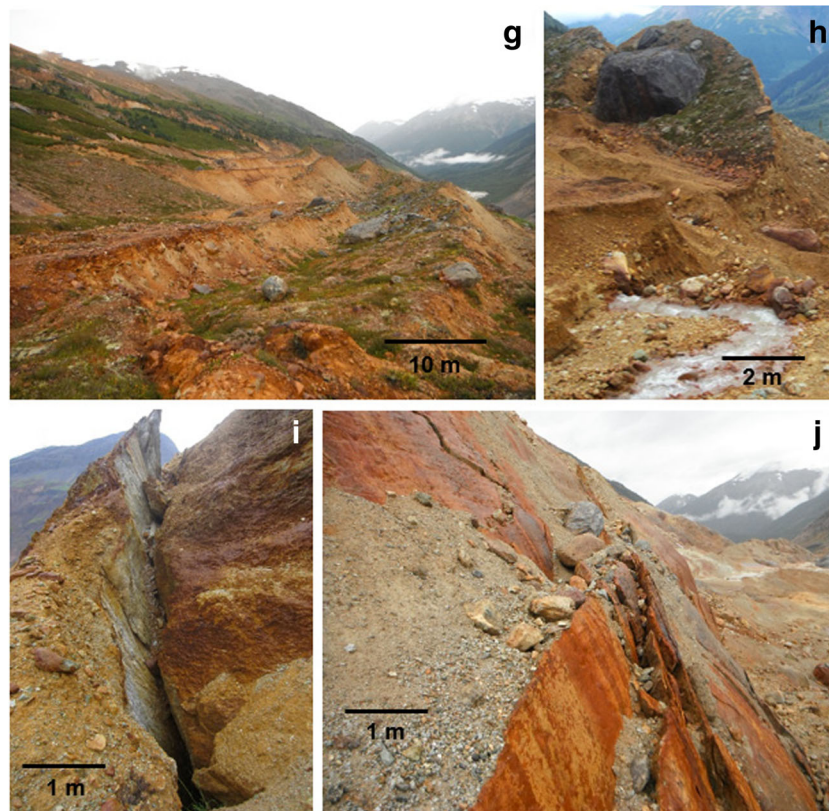


**Fig. 6** (continued)

wall are generally stronger with less alteration than those on the south wall (BGC 2010) and foliation dips into the slope, which also increases the stability of these slopes relative to the southern slope. On the south valley wall, a more than 100-m-wide band of more variable slope angle (increased roughness) is present at the elevation of the toppling/transition domain boundary. In Fig. 7, areas of the landslide that consistently have a higher than average roughness include the gully within the sliding block that ends in a fan on the mid-slope bench, the eastern half of the transition domain, and, in 1992 and 2010, the eastern corner of the toppling zone; this area is covered by glacial ice in 1956 so a comparison cannot be made for that time. On the maps of the MCL from 2010 (Fig. 4a–d) major scarps defining the edges of the landslide domains can be identified. The landslide back scarp and boundary between the upper sliding domain and transition domain can be clearly identified in the slope angle roughness map from 2010 (Fig. 7c) but are less well defined in the slope angle roughness map from 1992 (Fig. 7b), and are not visible in the slope angle roughness map from 1956 (Fig. 7a). The boundary between the upper instability and surrounding intact slope cannot be seen in the slope angle roughness maps.

### Deformation features

#### Timing and evolution

Evolution of the deformation feature network at the MCL between sets of photographs provides insight into the movement processes active at various stages of landslide development. Photographs of

typical deformation features and morphology of the zones are shown in Fig. 6. The set of major features that define landslide zones is present in all the photographs where surface deformation is visible (1972, 1992, and 2010) (Fig. 8). In 1992, a nearly threefold increase in visible deformation features is observed: with cracks identified in 1972 growing both in length and width, and new cracks forming between the major structures. The most recent set of photographs, from 2010, continues to show additional movement along approximately east-west striking foliation-parallel structures, and division of blocks of the landslide by minor features between, intersecting, and cross-cutting the major structures. The increase in length of deformation features is much reduced for this 18-year period; in 2010, the total length increased 50% from that observed in 1992. In contrast, displacements accommodated along deformation features during this period visibly increased the height and width of major scarps. Each of these time steps in the observed history of the MCL show a different stage in the development of the landslide, which remains juvenile and rapidly changing when compared to other large rock landslides, e.g., Downie Slide, which may have experienced movement over a millennium and has a mature deformation style (Kalenchuk 2010).

#### Feature orientation

The orientation of major toppling features is consistent throughout landslide development. In 1972, there are two sets (Fig. 9): the main one striking parallel to foliation at  $070\text{--}250^\circ$  and a minor set in the northeast corner striking  $120\text{--}300^\circ$ . In 1992, features in the dominant toppling orientation continue to develop and no new features are visible in the minor second orientation. By 2010, the



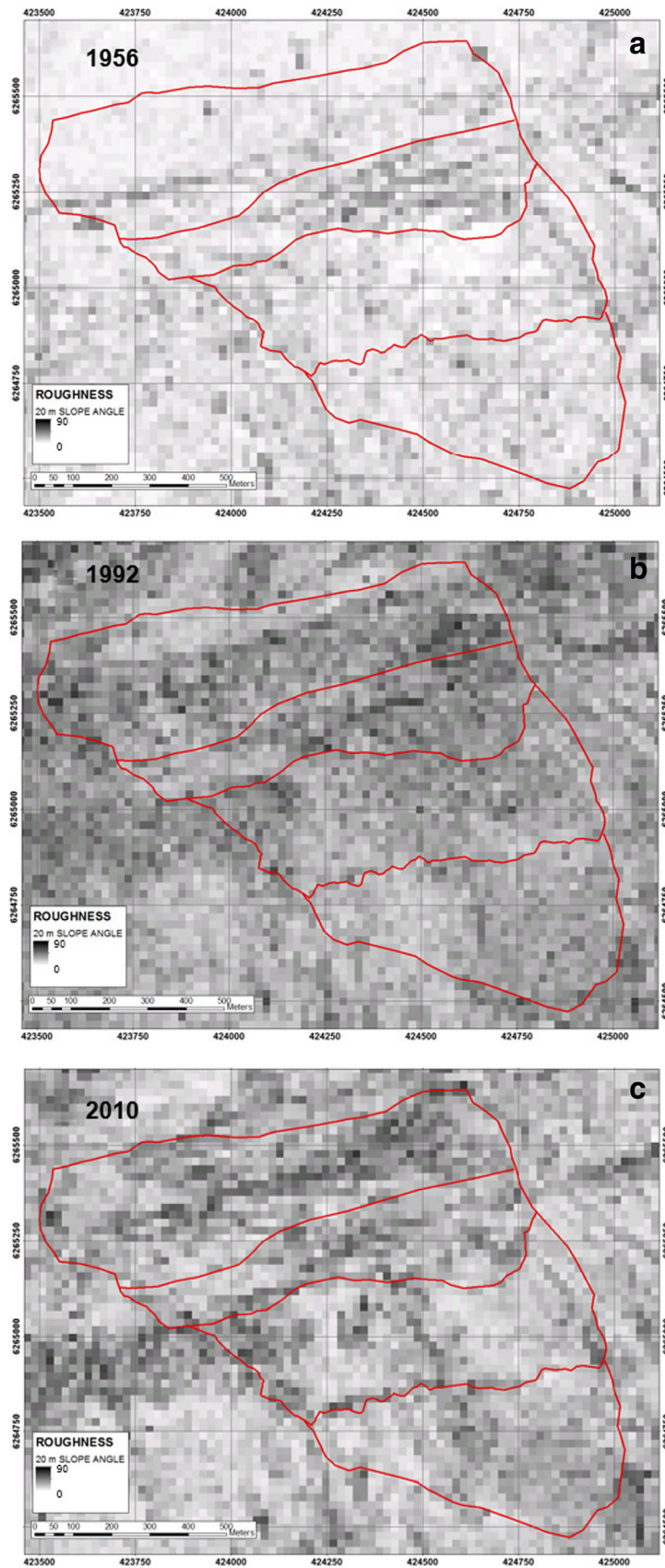


**Fig. 7** Block Statistics Slope Angle Roughness Maps for the MCL in a 1956, b 1992, and c 2010 with  $20 \times 20$  m blocks. *Red lines* delineate the landslide extents and geomorphic zone boundaries



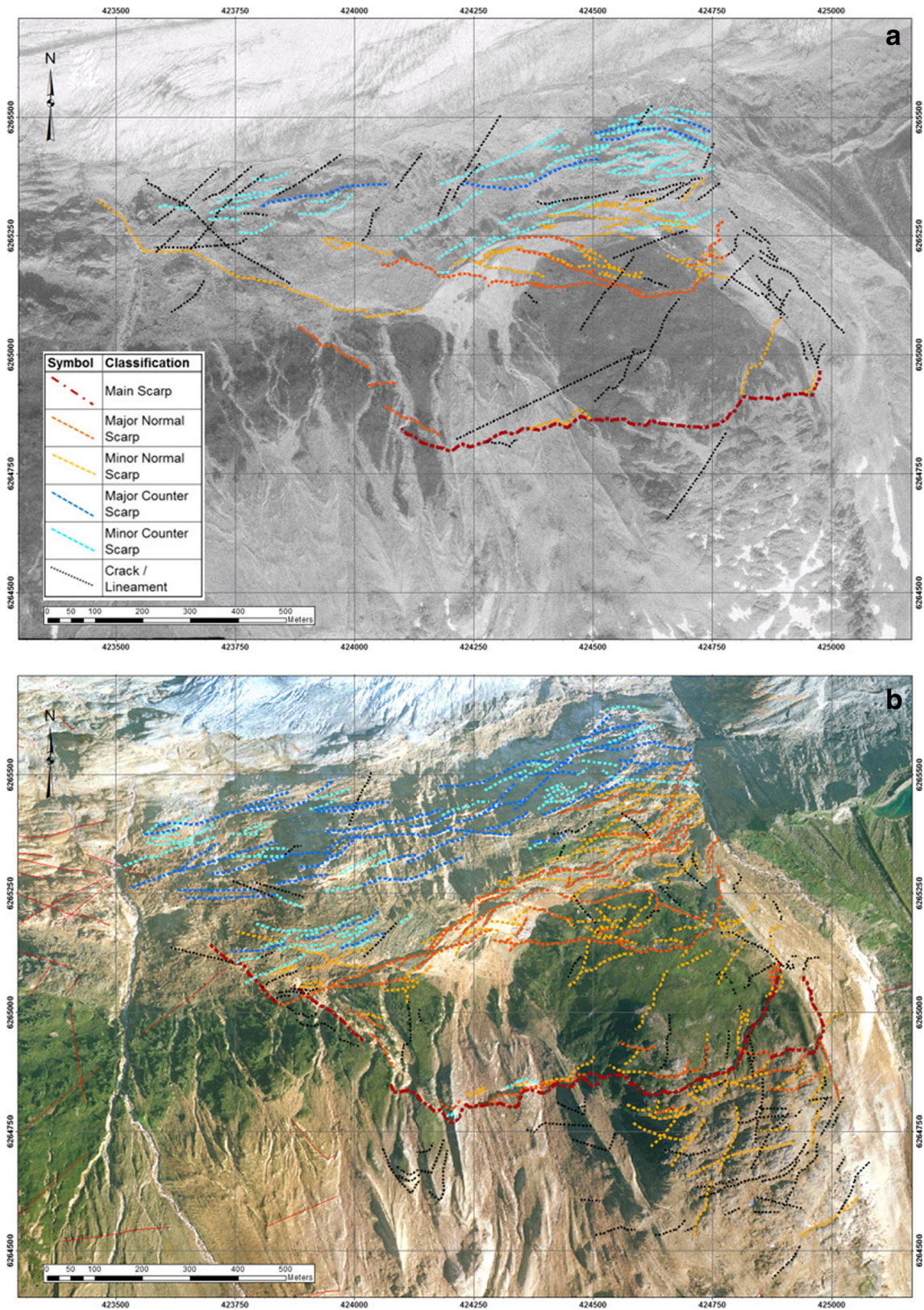
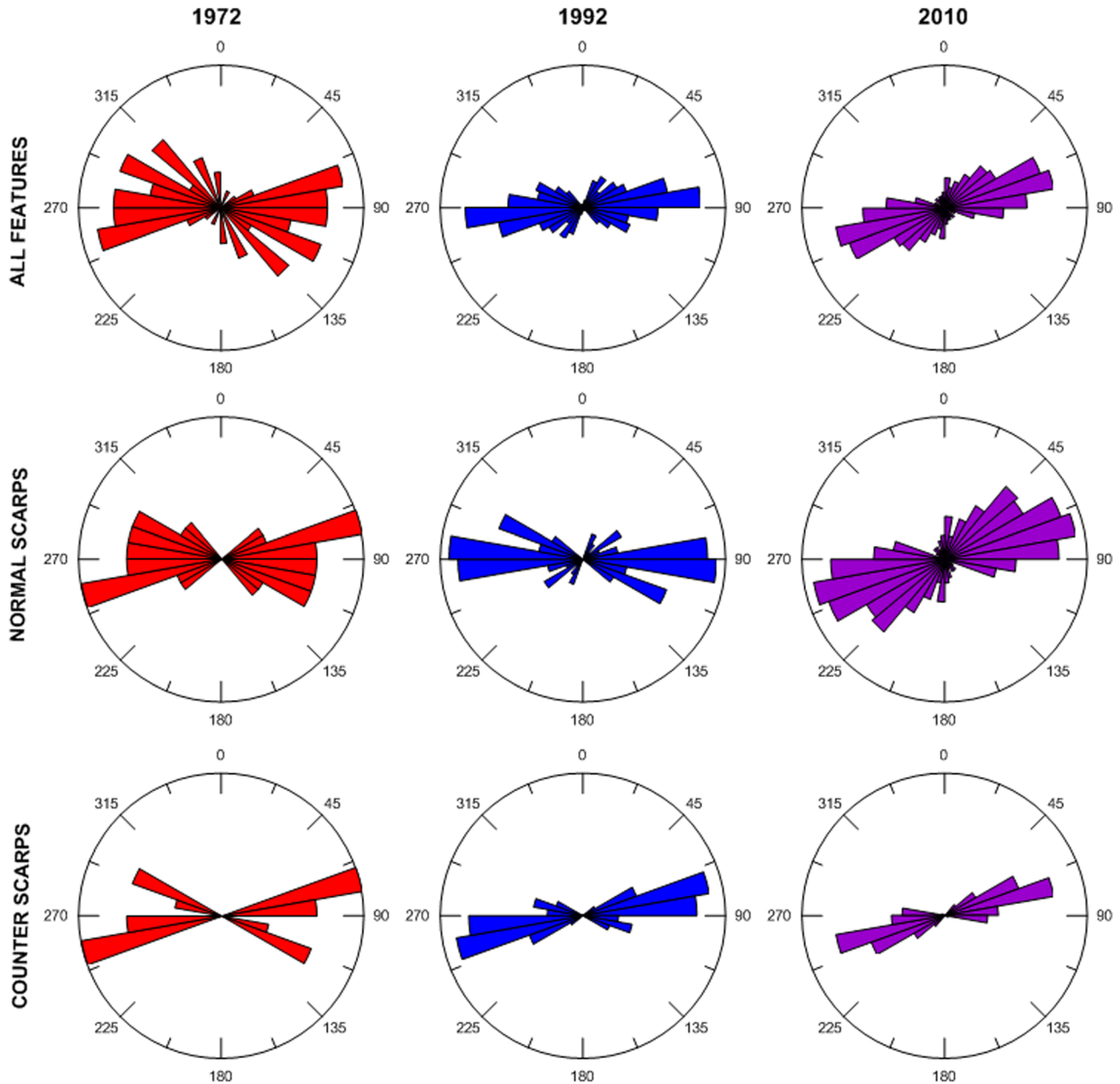


**Fig. 8** Landslide deformation features: a 1992, b 2010

secondary set is no longer distinguishable within the mapped features because the northeast corner of the zone is highly

disturbed. This area is covered in talus sourced from the landslide which obscures the features. The increased mobility of these



Dataset	All Features		Normal Scarps		Counter Scarps		Unclassified	
	Count	Length (m)	Count	Length (m)	Count	Length (m)	Count	Length (m)
1972	45	5,800	15	2,000	8	1,000	22	2,800
1992	172	17,100	65	6,300	60	5,500	47	5,300
2010	390	30,900	199	15,200	95	9,800	96	5,900

Fig. 9 Rosette plots and tabular summary of deformation feature strike classified by age and type

blocks compared with the remainder of the toppling zone may be a result of the intersecting toppling sets, the proximity of both the Mitchell Thrust fault and Brucejack fault, and its

location at a change in direction of  $40^\circ$  in the path of the Mitchell Glacier, all of which contribute to increased kinematic freedom.



Deformation features with a normal sense of movement show a changing dominant orientation. In 1972, the features present strike with a mean orientation of 090–270°; in 1992, the mean orientation is the same with less scatter as more features open up in the landslide mass. Between 1992 and 2010, there is an apparent rotation in the orientation of the primary normal scarps to 070–250° with a larger amount of variation in the orientation of the scarps from 1992. The 2010 deformation feature network is more complex than that of 1992, with interference between features beginning to show at the surface. In addition, by 2010, features are beginning to develop above the main landslide backscarp—which may indicate ongoing retrogression of the instability.

#### Geomorphologic zone

Within the toppling zone, there are several types of important features. First, the major scarps that cross from one side of the landslide to the other are spaced at approximately 50 m in both the 1992 and 2010 imagery. In 2010, these scarps have been split in places by other deformation features, and interference patterns between features are developing; connection of the scarps is still however identifiable (Fig. 8b). Minor scarps between these are spaced at approximately 25 m in 2010 with lengths ranging from 25 to 150 m. In 1992, there were only a few minor scarps, and they are typically less than 50 m long. The spacing of major counterscarp features in the toppling region in 2010 is estimated at 50 to 60 m, with lengths ranging from 100 to 400 m. In 1992, counterscarp features in the same region have an estimated spacing of 30 to 45 m, with similar length ranges 100 to 300 m. This indicates that there are toppling features that were visible in 1992 that have been destroyed or obscured in the intervening 18 years.

The only lineaments visible in the sliding block are oriented diagonally across the landslide, striking 030–210° (Fig. 9), approximately parallel to regional thrust faulting, and they have minor surface expressions—they do not appear to have experienced significant deformation. However, this group of structures may be important to landslide motion, as part of the main backscarp is oriented parallel to them, and a portion of the scarp dividing the transition zone from the sliding zone also follows this trend. Spacing of these lineaments ranges from 80 to 150 m; surface expression of the features is discontinuous, but most can be traced intermittently 0.5 to 1.0 km across the slope. It can be hypothesized that the sliding block has experienced a relatively small amount of internal deformation compared with the transition and toppling zones.

Above the main backscarp in the potentially retrogressing instability there are two main lineament orientations, one parallel to regional foliation and spaced 25 to 40 m apart is 50 to 250 m long in 2010, and does not appear to have experienced deformation in 1992. Intensity of deformation across these features appears to increase with proximity to the landslide. The second group is parallel to the strike of regional faulting; with a spacing of approximately 60 m, and length ranging from 100 to 250 m.

#### Point displacement monitoring

Displacement monitoring is a crucial part of understanding the behavior of large bedrock slides. Movement rates and deviations from established normal behavior can provide insight that might signal stabilization of the slide mass, or acceleration towards catastrophic failure. At the Mitchell Creek Landslide, a nearly 60-

year record of movement can be extracted from historic aerial imagery. Temporal variations in displacement between photographs could not be evaluated, as it is possible that the landslide experienced large variability in annual rates of movement. Due to ice cover in 1956, few targets could be selected in the toppling zone, leading to a lack of data from the lower half of that zone. An estimated rate of 2 m/year ice loss has been observed on the Mitchell Valley Glacier.

The highest degree of variation in displacement rates is observed in the toppling zone; this is consistent with expectations for a zone with complex deformation processes. Slabs within the toppling rock mass may move independently of each other. In 2013, large (>5 m across) hung-up blocks were observed in the toppling zone. The base of this zone coincides with the footwall of the MTF; tectonic damage could be expected in a zone around the fault which could lead to more rapid ground movement than in the less damaged rocks above. The average rate of movement in the toppling zone from 1956 to 2010 is 0.8 m/year, with a range of approximately 0.5 to 1.5 m/year. The high horizontal displacement estimates for this zone appear to disagree with point cloud comparisons as they do not consider vertical displacement and the closest point algorithm only identifies slope morphology changes.

The transition zone has a slower estimated plan displacement rate than the toppling zone, at an average of 0.33 m/year with less variation between points. This block is interpreted to represent a complex zone between primarily sliding rock above and toppling below, it is down-dropping, extending, and may be contributing gravitational driving forces pushing the toppling zone outwards. It may also be simply subsiding into the space created from primary toppling in the slope below.

The sliding zone displacement rates are slower again than the transition zone, with average annual movements of 0.19 m/year. This zone covers the upper third of the landslide slope, and is interpreted to be sliding along a geologically controlled basal rupture surface as a relatively intact block that was initially a retrogressive part of the landslide that began in the steep toppling slope. Slow movement rates are consistent with this interpretation.

Tracking movement in the potentially retrogressing upper block was unsuccessful, for a number of reasons. First, the expected movements are quite small compared with movements of the main landslide. Second, the onset of movement in the zone is unclear from the photographs but was likely after significant movement of the main slide had occurred. Third, there is partial snow cover of the outcrops in this zone in older photographs obscuring landmarks used for georeferencing. And finally, in 1992, this zone is at the edge of the photographs where there is some image distortion that the georeferencing process used could not remove.

Annual surface displacement rates and azimuths from 2008 to 2013 are in general agreement with the average rates estimated between 1956 and 2010 (Table 4). Estimated movement rate in the toppling zone is lower in survey data, but this is likely due to the location of the survey points, which are primarily in the upper part of the zone which was observed to be moving slower than the lower toppling zone in the historic imagery. Consistency between annual displacement rates estimated from historic photographs and geotechnical monitoring indicates that landslide behavior has not significantly varied from year to year over the recorded time interval.

Table 4 Summary of landslide monitoring data

Monitoring interval	Data source	Sliding zone Displacement rate (m/year)	Azimuth	Number of points	Transition zone Displacement rate (m/year)	Azimuth
1956–2010	Aerial photography	0.19	350	20	0.33	342
2008–2013	Point surveys	0.14	330	5	0.35	336
Monitoring interval	Transition zone Number of points	Toppling zone Displacement rate (m/year)	Azimuth	Number of points	Glacial downwasting (m/year)	
1956–2010	17	0.80	350	10	2	
2008–2013	6	0.42	341	4	N/A	

### Discussion and conclusions

This paper summarizes the results of a detailed surficial characterization of the Mitchell Creek Landslide using aerial photography, field data, and GIS analysis techniques. Applying digital photogrammetry techniques to historical aerial photographs allowed for detailed analysis of approximately 20-year time steps through the development of the Mitchell Creek Landslide. This study highlights the usefulness of historical aerial photographs applied to long-term landslide evolution. The 1956 model provided a pre-failure state for the slope to compare to the current state of the landslide. Comparisons between the subsequent models provided insight into landslide movement magnitudes and direction; the large displacements experienced at the MCL (up to 50 m between 1956 and 2010) far exceed model generation uncertainties.

The detailed interference map generated from 1992 and 2010 point cloud data (Fig. 3) provides further insight into landslide movement style. A clear division between the sliding block and transition zone is apparent, as is the change from subsidence to slope bulging at the top of the toppling zone. The division between the sliding and transition domains occurs along a discrete major scarp visible in the aerial photographs. In the western region of the landslide, movement along this scarp is clear between 1992 and 2010, while in the eastern region of the landslide it is not as obvious. The division between transition and toppling occurs on a number of major scarps at approximately the same level across the landslide, where the displacement character abruptly changes. Beginning at the top of the landslide, sliding along the basal shear surface has resulted in down-dropping of 2 to 5 m at the backscarp. Displacement of the mid sliding zone has not resulted in significant subsidence, or lowering of the ground elevation, because of the interaction of pre-existing topography and block movement along the planar upper landslide failure surface. As the slope moves northwards, the surface elevation remains unchanged because the sliding slab has a consistent thickness in this area and it is sliding as an intact block along a discrete failure surface. In the transition zone, the largest amount of subsidence occurs on the moraine ridge with slightly greater than 20 m of change near the middle of the slope, and between 10 and 15 m on average for the ridge. In the toppling zone, bulging occurs across the entire width of the landslide with magnitudes of change ranging from 5 to 15 m. This is consistent with initial conceptual models for landslide motion (BGC Engineering Inc. 2012) and observations from the DTM difference map shown in Fig. 2.

Using engineering geomorphology mapping techniques (Geological Society of London 1982, Griffiths 2002; Wolter 2014), slope angle and aspect, geologic and glacial history of the slope and their impact on landslide development were considered. Retreat of the Mitchell Valley glacier appears to have played a role in landslide initiation: as the ice mass receded the slide was kinematically free to displace into the valley. Morphological maps allow for quick visual assessment of slope changes since onset of landsliding. Geomorphic zones were delineated based on the current landslide geometry—these zones have changed little over the documented history of the MCL.

Deformation features were identified and interpreted through time, providing insight into landslide initiation and controlling mechanisms. Linkages between surface deformation and structural geology were assessed. Strike orientations measured from deformation features within the MCL are generally east-west, parallel



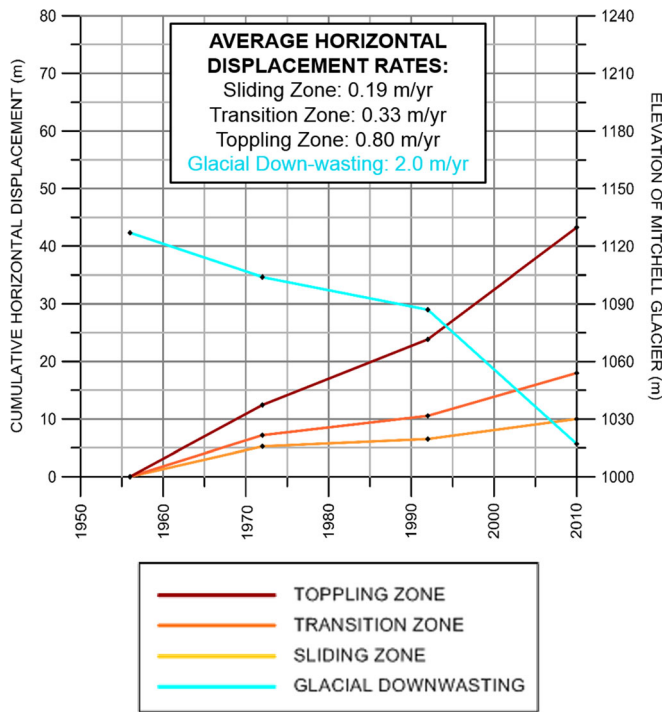


**Fig. 10** Average point displacement tracking results for each landslide domain from 1956 to 2010

to regional foliation in all geomorphic zones. Above the main landslide, opening and relaxation is occurring along geologic structures, especially 070 to 090° striking foliation, and sinkholes are developing at the intersection of these opening structures. In the sliding block, the main visible feature is the backscarp; evidence of surface water flow into the backscarp and other deformation features was observed in the field, with at least one major stream fully diverted to subsurface through an open normal scarp. Vegetation covers small-scale features that are present in this zone. The mid-slope transition block is covered by glacial sediments, in places over 10 m thick, and deformation is visible along many large scarps. Benches between scarps that dip counter to the main slope direction are intact pieces of the Mitchell Glacier's Little Ice Age (LIA) lateral moraine, and have not been back-rotated. Within the toppling block, foliation is rotating out of the slope and large slabs have broken off from the slope. The zone is covered by a thin, discontinuous blanket of ablation sediments. Large talus aprons composed of landslide debris and glacially transported material have developed at the base of the toppling zone. The MTF and tectonic damage associated with it which intersects the lower landslide slope likely controls the lower limit of landslide movement. On the eastern side of the MCL, the tributary glacier valley, which itself follows the Brucejack normal fault, provides a lateral release for the landslide. The intersection of the MTF and BJF occurs at the base of the northeast corner of the landslide (Fig. 1), as does a bend in the path of the Mitchell Glacier; the

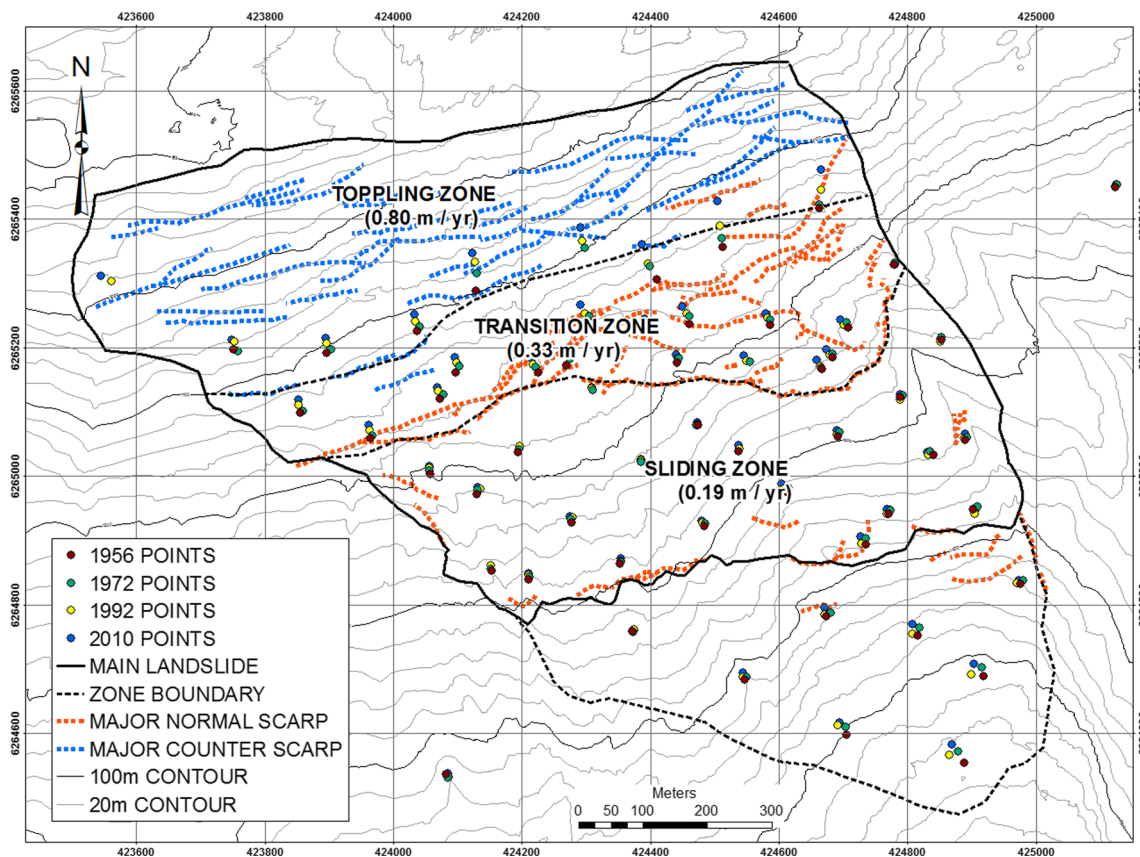


**Fig. 11** Summary engineering geomorphology map of the Mitchell Creek Landslide. Major scarps and average displacement rates for each geomorphic zone indicated

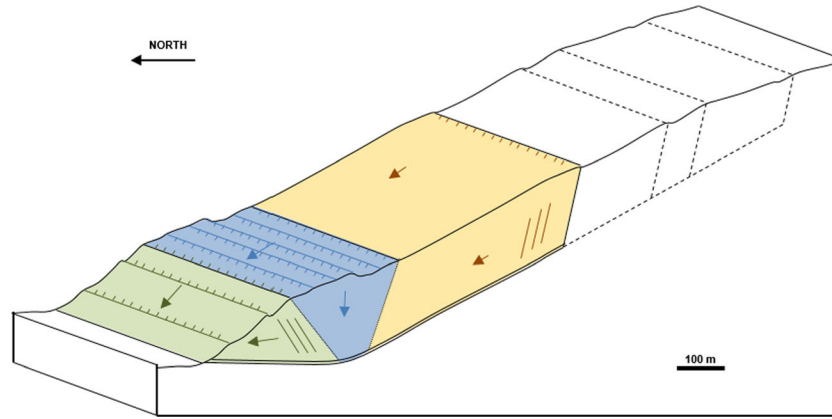


**Fig. 12** Conceptual model of the MCL showing geomorphic zones, toppling in *green*, transition in *blue*, sliding in *yellow*, and the upper instability as relaxing blocks above the main landslide. Foliation orientation in the toppling and sliding blocks is indicated in the cross section view

combination of increased potential for glacial plucking and lateral release at the BJT may be responsible for the greater degree of disintegration of the rock mass at surface observed there.

The deformation features observed at surface can provide some insight into the three-dimensional behavior of the landslide. Areas with a higher intensity of deformation features have likely experienced more internal deformation than areas with few features, and the size of intact blocks and columns within the landslide mass are controlled by the location and intensity of internal shearing.

Natural point tracking on aerial photographs has provided a baseline of movement rates for the MCL beginning in 1956—prior to the onset of landslide motion, which future measured rates can be compared against. Average rates of landslide movement have been remarkably consistent over the last 60 years. An apparent connection between minor changes in displacement rate and glacial downwasting can be seen in Fig. 10: where between 1972 and 1992 the slowest rate of ice loss coincides with the slowest average slope movement rate, and where from 1992 to 2010 a dramatic increase in glacial ice loss is observed and landslide movement rates also increase. The remaining glacial ice outboard of the landslide is below the base of the unstable rock mass; it is therefore no longer providing any kinematic restraint and further downwasting and retreat should have no additional effect on the landslide.


Figure 11 summarizes the engineering geomorphological model, highlighting major scarp features (as of 2010), geomorphic zones, and displacement rates. Surficial assessment of the MCL using engineering geomorphology and GIS analysis identified major movement mechanisms active within the slope. In the lower slope, there is structural toppling resulting in compression and bulging of the rock mass. The mid-slope transition is down-dropping and may be driving movement of the lower slope, failing into the space behind the lower toppling slope or a combination of the two as landslide movement continues. Extensional deformation features are present particularly in the upper portion of this zone that indicate the zone is moving away from the sliding block above. The uppermost section of the MCL is undergoing translation as it continues to move downwards along a structurally controlled rupture surface as a relatively intact block. Above the main landslide, secondary instability is developing as support is removed

through downslope movement of the sliding block. Figure 12 illustrates the conceptual model of landslide behavior, combining the geomorphological zones and observed scarps with movement style and subsurface interpretations. A very useful aspect of the MCL is that historical aerial photographs of the site were captured at approximately 20-year intervals with the oldest photograph from prior to the onset of failure—allowing for interpretation of a complete model of landslide development.

## References

- Adam Technology Inc. 2012. 3DM CalibCam and 3DM Analyst. Version 2.5.0 Build 1114 32-bit. Software and user manuals. Available from: <http://www.adamtech.com.au>
- BGC Engineering Inc., 2010. KSM Project: Mitchell Zone—open pit slope design—final. Submitted to Seabridge Gold Inc., 2010
- BGC Engineering Inc., 2012. KSM Project—preliminary geotechnical assessment of the Snowfield Landslide—final. Submitted to Seabridge Gold Inc., 2012
- Bovis M (1990) Rock-slope deformation at Affliction Creek, southern Coast Mountains, British Columbia. *Canadian Journal of Earth Science* 27:243–254
- Campbell, KV 2009. Review of structural geology in relation to preliminary structural domains. Submitted to BGC Engineering Inc., 2009
- Clague JJ, Stead D (2012) *Landslides: types, mechanisms and modelling*—preface. Cambridge University Press, New York
- Cruden DM, Varnes DJ (1996) Landslide types and processes. In: Turner AK, Schuster RL (eds) *Landslides investigation and mitigation*, Special Report 247 edn. Transportation Research Board, US National Research Council, Washington, DC, pp 36–75
- Division of Engineering and Geoscientists in the Forest Sector (DEGIFS), 2002. A user's guide to terrain stability mapping in British Columbia. 89 pages. Prepared for APEGBC, 2002
- ERSI, 2013. ArcGIS software. <http://www.esri.com/>
- Geological Society of London (GSL): Engineering Group Working Party (1972) The preparation of maps and plans in terms of engineering geology. *Q J Eng Geol* 5:297–367
- Giardino M, Giordan D, Ambrogio S (2004) G.I.S. technologies for data collection, management, and visualization of large slope instabilities: two applications in the Western Italian Alps. *Nat Hazards Earth Syst Sci* 4:197–211
- Griffiths JS (2002) Mapping and engineering geology: introduction. From: mapping in engineering geology. *The Geological Society. Key Issues in Earth Sciences* 1:1–5
- Griffiths JS (2014) Feet on the ground: the past, present and future of engineering geology—the Fourteenth Glossop Lecture. *Quarterly Journal of Engineering Geology of Engineering Geology and Hydrogeology* 47:116–143



- 
- Hencher SR, Malone AW (2012) Landslides: types, mechanisms and modelling—chapter 30: Hong Kong landslides. Cambridge University Press, New York
- Hungr O, Leroueil S, Picarelli L (2014) Varnes classification of landslides types, an update. *Landslides* 11:167–194
- InnovMetric Software Inc., 2013. Polyworks, version 12.0.17 build 5761 <http://www.innovmetric.com>
- Kalenchuk KS, 2010. Multi-dimensional analysis of large, complex slope instability. PhD thesis, Queen's University, Kingston, Ontario, Canada. 449 pages
- Lechner MJ, 2008. Updated Mitchell Creek technical report, Northern British Columbia. Resource Modelling Inc
- Margolis, J. 1993. Geology and intrusion-related copper-gold mineralization, Sulphurets, British Columbia (PhD dissertation). University of Oregon, Eugene, 289p, 5 maps
- Rescan Environmental Services Ltd., 2009. KSM Project 2008. Baseline studies report. submitted to Seabridge Gold Inc. 2009
- Schwab JW, Geertsema M (2010) Terrain stability mapping on British Columbia forest lands: an historical perspective. *Nat Hazards* 53(1):63–75
- Stead D, Clayton A (2014) Evaluation of development of the Mitchell Creek Landslide, B.C., using Remote Sensing, Geomorphological Analysis and Numerical Modelling. American Geophysical Union, Fall Meeting 2014, abstract #NH43A-3796
- Turner AK, 1996. Landslides: investigation and mitigation. Transportation Research Board Special Report 247
- Wolter A (2014) Characterisation of large catastrophic landslide using an integrated field, remote sensing, and numerical modelling approach (PHD dissertation). Simon Fraser University, Burnaby, p 323
- 
- A. Clayton**  · **D. Kinakin**  
BGC Engineering Inc.,  
980 Howe St, V6Z 0C8, Vancouver, BC, Canada  
e-mail: [aclayton@bgcengineering.ca](mailto:aclayton@bgcengineering.ca)
- D. Stead**  
Simon Fraser University,  
8888 University Dr, V5A 1S6, Burnaby, BC, Canada
- A. Wolter**  
ETH Zurich,  
Sonneggstrasse 5, 8092, Zürich, Switzerland